

Scaling analysis of transverse Anderson localization in a disordered optical waveguide

Behnam Abaie and Arash Mafi*

Department of Physics & Astronomy, University of New Mexico, Albuquerque, NM 87131, USA
Center for High Technology Materials, University of New Mexico, Albuquerque, NM 87106, USA

(Dated: December 9, 2024)

The intention of this manuscript is twofold. First, the mode-width probability density function (PDF) is introduced as a powerful statistical tool to study and compare the transverse Anderson localization properties of a disordered one dimensional optical waveguide. Second, by analyzing the scaling properties of the mode-width PDF with the transverse size of the waveguide, it is shown that the mode-width PDF gradually converges to a terminal configuration. Therefore, it may not be necessary to study a real-sized disordered structure in order to obtain its statistical localization properties and the same PDF can be obtained for a substantially smaller structure. This observation is important because it can reduce the often demanding computational effort that is required to study the statistical properties of Anderson localization in disordered waveguides. Using the mode-width PDF, substantial information about the impact of the waveguide parameters on its localization properties is extracted. This information is generally obscured when disordered waveguides are analyzed using other techniques such as the beam propagation method. As an example of the utility of the mode-width PDF, it is shown that the cladding refractive index can be used to quench the number of extended modes, hence improving the contrast in image transport properties of disordered waveguides.

PACS numbers: 42.25.Dd, 42.82.Et, 72.15.Rn

I. INTRODUCTION

Anderson localization has been a topic of great scientific interest for over five decades^{1–3}. It has been successfully demonstrated in highly scattering classical wave systems including acoustics^{4,5}, electromagnetics⁶, optics^{7–13}, as well as quantum optical systems, such as atomic lattices¹⁴ and propagating photons^{15–18}. Transverse Anderson localization of light was first suggested by Abdullaev, et al.¹⁹ and De Raedt, et al.²⁰ and was confirmed experimentally by Schwartz, et al.²¹. In particular, De Raedt, et al. analyzed an optical waveguide with a transversely random and longitudinally invariant refractive index profile. They showed in this quasi-two-dimensional (quasi-2D) system that an optical beam can propagate freely in the longitudinal direction while being trapped (Anderson localized) in the transverse direction. Transverse Anderson localization of light has since been observed in various quasi-one-dimensional (quasi-1D) and quasi-2D optical systems^{22–27}.

Most recently, Karbasi, et al. reported the first observation of transverse Anderson localization in disordered optical fibers^{25–27}. The disordered optical fibers were used for image transport²⁸ and it was shown that the high quality image transport was achieved because of, not in spite of, the high level of disorder and randomness in the fiber^{28,29}. A high-quality imaging optical fiber based on transverse Anderson localization requires a *narrow* and *uniform* point spread function (PSF) across the tip of the fiber. The width of the PSF is determined by the localization radius; it has been argued that a large refractive index contrast is essential in ensuring that the localization radius is *sufficiently small* and *does not vary appreciably* across the fiber profile^{26–28}. The large refrac-

tive index fluctuations of around 0.1 in the disordered polymer fiber by Karbasi, et al. ensured a *strong* and *uniform* transverse localization across the tip of the fiber for high quality image transport.

A disordered waveguide can support both localized and extended modes simultaneously. Because the refractive index of a disordered waveguide is random, the properties of the localized and extended modes should be studied using statistical techniques. The most relevant physical quantity that characterizes the localization properties of disordered waveguides is the mode width. Therefore, detailed understanding of the *mode-width statistics* is the gateway to uncovering the localization properties. In this manuscript, we report on the *probability density function* (PDF) of the mode width as a powerful tool to study Anderson localization in disordered waveguides. Using the *mode-width PDF*: we can obtain the average width of the localized modes which determines the size of the PSF for a disordered imaging fiber; we can obtain the standard-deviation of the mode-width distribution which determines the uniformity of the transported image across the tip of the fiber; we can obtain the distribution of the extended modes which affect the image contrast; and we can study the impact of the total size of the structure and the cladding index contrast on the localized and extended modes.

The mode-width PDF contains all the relevant information on the mode-width statistics of a disordered waveguide ensemble. However, computing the mode-width PDF is a challenging numerical problem. In order to compute the PDF, a large number of different waveguide samples are generated in a given ensemble for proper statistics. The guided modes for each waveguide are calculated and the corresponding mode-width values are extracted to generate the PDF. Calculating the

guided modes of even a single fiber structure may become highly challenging. For example, the V-number of the disordered polymer fiber in Ref.²⁵ with air cladding is approximately 2,200 at 405 nm wavelength resulting in more than 2.3 million guided modes²⁵. Solving for all these modes for a given fiber and obtaining proper statistical averages over many fiber samples is a formidable task even for large computer clusters. However, a mode-width PDF is an absolutely necessary tool if one wants to obtain proper understanding of the behavior of the localized modes as well as the extended modes and their interaction with the fiber boundary. In this manuscript, *we employ the power of scaling analysis* and study the mode-width PDF as a function of the total size of the waveguide. We show that the PDF converges to a terminal form as the waveguide dimensions are increased. As such, the mode-width PDF of a real-sized disordered waveguide may be obtained by simulating a waveguide ensemble of a considerably smaller dimensions. Moreover, we will show that the region of the PDF corresponding to the Anderson localized modes converges to its terminal form considerably faster than the entire PDF as the size of the structure grows larger, while the region of the PDF corresponding to the extended modes is rather generic looking. Therefore, to obtain the most useful information corresponding to the Anderson-localized region of the PDF, it is often possible to even further reduce the size of the structures resulting in substantial reduction in computational effort. In certain systems, this may actually turn the computational problem from nearly impossible to one that can be handled by moderate sized computer clusters.

The focus of this manuscript is to establish a framework for a comprehensive analysis of the mode-width statistics for transverse Anderson localization in optical fibers in the future. A mode-width distribution that is more strongly peaked at narrower mode-width values is favored because it can result in a smaller PSF for imaging applications. Moreover, a narrower distribution of the mode-widths indicates PSF uniformity across the fiber. In order to lay the groundwork for understanding the scaling behavior of the statistical distribution for both the localized and extended modes in a 2D Anderson localizing optical fiber, we have decided to present a comprehensive characterization of a 1D Anderson localized optical waveguide in this manuscript. This exercise is quite illuminating as it sheds light on the scaling behavior of the statistical distribution of the mode widths and shows the extent of information that can be extracted from such an exercise. The detailed analysis of a 2D disordered fiber structure will be presented in a future publication.

Here, we have chosen to calculate the transverse electric (TE) guided modes of the disordered waveguide using finite element method (FEM) presented in Refs.^{30–34}. Similar observations can be drawn for transverse magnetic (TM) guided modes, but we limit our analysis to TE in this paper for simplicity. For each guided mode,

the mode width is defined as the standard deviation σ_2 of the normalized intensity distribution $I(x)$ of the mode according to

$$\sigma_2 = \left(\int_{-\infty}^{+\infty} (x - \bar{x})^2 I(x) dx \right)^{1/2}, \quad (1)$$

where the mode center is defined as

$$\bar{x} = \int_{-\infty}^{+\infty} x I(x) dx. \quad (2)$$

x is the spatial coordinate across the width of the waveguide and the mode intensity profile is normalized such that $\int_{-\infty}^{+\infty} I(x) dx = 1$. σ_2 is a measure of width of the modes i.e. a larger σ_2 signifies a wider mode intensity profile distribution.

Finally, we would like to contrast the power of the statistical simulation in the modal method with that of the finite difference beam propagation method (FD-BPM)³⁵ employed earlier in Refs.^{21,26}. When using the FD-BPM to analyze the Anderson localization in optical waveguide, one is always worried about the extent to which the results are dependent on the shape and size of the input beam. The modal description is superior because it relies solely on the physics of the disordered system and is independent of the properties of the external excitation³⁶. As it will be shown in this manuscript, the mode-width PDF can reveal the subtle interplay between Anderson localized modes, conventional waveguided modes, and non-localized extended modes, all of which can be present simultaneously in a disordered waveguide—something that cannot be achieved using the FD-BPM analysis.

II. 1D DISORDERED LATTICE INDEX PROFILE

A 1D ordered optical lattice can be realized by periodically stacking dielectric layers with different refractive indexes on top of each other. Fig. 1(a) shows the refractive index profile of a periodic 1D optical waveguide where n_0 , n_1 , and n_c correspond to the lower index layers, higher index layers, and cladding, respectively. In order to make a disordered waveguide, randomness can be introduced in different ways in the geometry or refractive index profile of a waveguide structure. For example, in Refs.^{34,36} the thickness of the layers is randomized around an average value. In this manuscript, we adopt a different randomization method: we keep the thickness of all dielectric layers identical but assign a refractive index value of n_0 or n_1 to each layer with a 50% probability. This is the same as the method prescribed by De Raedt, et al.²⁰ in randomizing a disordered 2D waveguide which was also adopted by Karbasi, et al.²⁵ to fabricate an Anderson localizing fiber. As we explained in the Introduction, our intention is to extend our current analysis to 2D disordered Anderson localizing fibers in the future and we

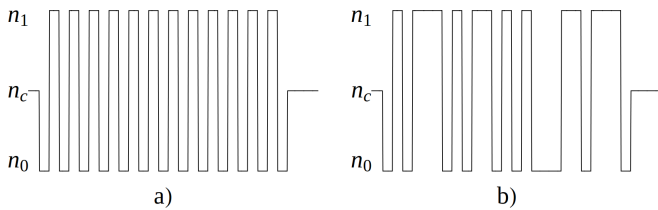


FIG. 1. Sample refractive index profiles of (a) ordered and (b) disordered slab waveguides are shown.

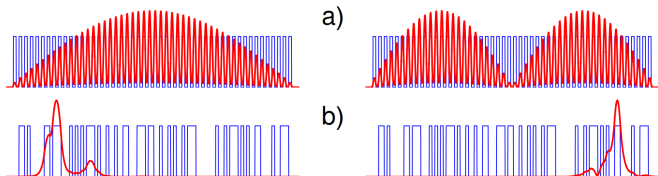


FIG. 2. Typical mode profiles for (a) an ordered slab waveguide where each mode extends over the entire waveguide, and (b) a disordered slab waveguide, where the modes are localized.

would like to stay as close as possible to the practical disordered 2D structure for proper comparison.

Fig. 1(b) shows the refractive index profile of a disordered 1D optical waveguide. In Fig. 2(a), we plot two guided modes of a 1D periodic waveguide with the highest propagation constant, where we have assumed that $n_0 = 1.49$, $n_1 = 1.50$, and $n_c = 1.49$. These two modes belong to a large group of standard *extended* Bloch periodic guided modes supported by the ordered optical waveguide, which are modulated by the overall mode profile of the 1D waveguide³⁶. The total number of guided modes depends on the total thickness and the refractive index values of the slabs and cladding. The key point is that each mode of the periodic structure extends over the entire width of the waveguide structure. A similar exercise can be done with a 1D disordered waveguide, where two arbitrarily selected modes are plotted in Fig. 2(b) using the same refractive index parameters as that of the periodic waveguide. It is clear that the modes become localized in the disordered 1D waveguide. While there are variations in the shape and width of the modes, the mode profiles shown in Fig. 2(b) are typical.

It is important to note that the disordered core of the lattice is sandwiched between a cladding with a refractive index of n_c that can also be adjusted to resemble experimental situations where a waveguide is surrounded by air or a dielectric with a refractive index higher than air or even n_0 (but always less than n_1 to ensure waveguiding). As we will see later, the value of n_c influences the mode-width distribution of the extended modes in a 1D Anderson localized waveguide and should be carefully studied in practical implementations of such structures, e.g. for image transport²⁸.

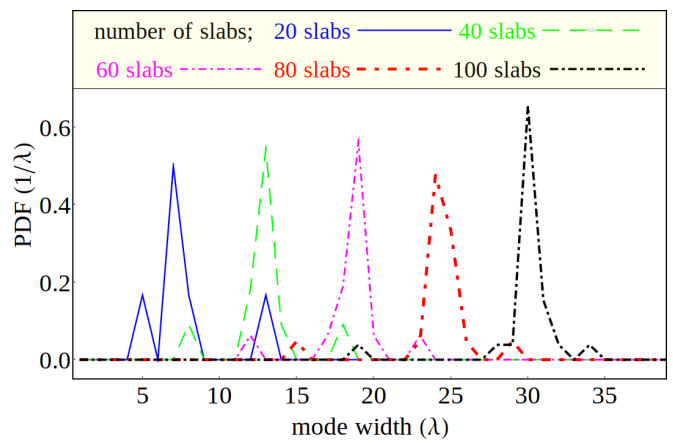


FIG. 3. Mode-width PDF of an ordered waveguide defined as $\Delta n_{\text{core}} = 0.01$ and $\Delta n_{\text{clad}} = 0$, for $N = 20, 40, 60, 80$, and 100 slabs. Mode width increases as the number of slabs increases, so the average mode width scales proportional to the size of the structure.

III. ANALYSIS OF THE MODE-WIDTH PDF

In the absence of localization, guided modes are Bloch periodic and extend over the entire width of a waveguide as shown in Fig. 2(a). In this case, the confinement is merely due to the total internal reflection at the effective index step between the waveguide and the cladding. In Fig. 3, we plot the mode-width PDF for the periodic waveguide with N slabs, for $N = 20, 40, 60, 80$, and 100 . The width of each slab is equal to the wavelength $d = \lambda$, $n_c = n_0 = 1.49$, and $n_1 = 1.50$ so the index step $\Delta n_{\text{core}} = 0.01$ where $\Delta n_{\text{core}} = n_1 - n_0$. The horizontal axis is in units of λ and the vertical axis is in units of $1/\lambda$ such that the PDF integrates to one (unit area under the PDF curve). The width of the cladding is assumed to be 25λ on each side of the waveguide. Figure 3 shows that for the periodic slab waveguide, the mode widths are determined by the width of the waveguide as can be seen clearly in Fig. 2(a). Therefore, the mode widths, on the average, scale linearly with the size of the waveguide structure and the peak of the PDF shifts to larger values of mode width as the waveguide becomes wider.

For a disordered waveguide, the scaling behavior of the PDF with the size of the waveguide is completely different from that of the periodic waveguide shown in Fig. 3. When Anderson localization comes into play due to the disorder in the structure of waveguide, most guided modes become transversely localized as shown in Fig. 2(b), while a few extended guided modes may still be supported depending on the waveguide configuration. As the number of slabs is increased, the PDF saturates to a terminal form. In Fig. 4, we show the PDF for an ensemble of disordered waveguides with N slabs defined by $n_c = n_0 = 1.49$, and $n_1 = 1.50$ ($\Delta n_{\text{core}} = 0.01$), where the width of each slab is equal to the wavelength $d = \lambda$. The PDFs are plotted for $N = 20, 40, 60, 80$, and

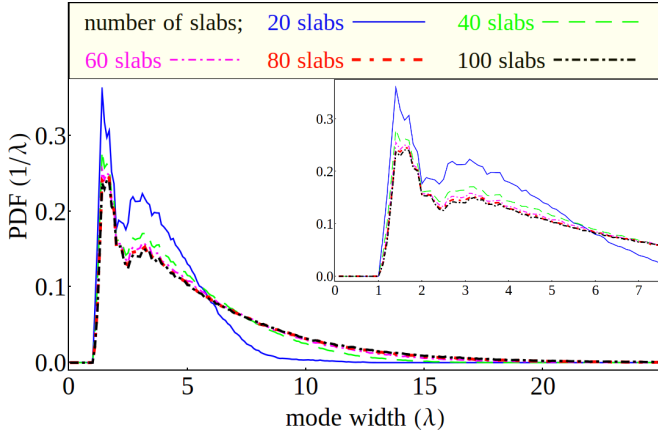


FIG. 4. Mode-width PDF of a disordered waveguide defined by $\Delta n_{\text{core}} = 0.01$, $\Delta n_{\text{clad}} = 0$, for $N = 20, 40, 60, 80$, and 100 slabs. The inset is the magnified version of the localized peaks of the PDFs. Saturation of the PDF beyond $N_{\text{sat}} \approx 60$ is clear in this figure.

100. The PDF shows two localized peaks at width values less than 4λ with a long tail signifying the extended modes. The shape of the PDF changes with the number of slabs; however, it remains nearly unchanged beyond $N_{\text{sat}} \approx 60$. The near saturation of the PDF beyond a critical number of slabs N_{sat} is of utmost importance for two reasons: 1) N_{sat} can be viewed as the effective transverse scale (waveguide width) beyond which the average localization dynamic is no longer dictated by the boundary; and 2) if we need to calculate the PDF for a wide disordered waveguide, it is sufficient to simulate a waveguide with only N_{sat} slabs because it gives the same PDF; therefore, the computational effort can be significantly reduced. In order to see the saturation behavior of the PDF more clearly, the inset shows a magnified version of the PDFs, which is zoomed in at smaller mode width values. The transition to the terminal form of the PDF is clearly observed in the Anderson localized region of the PDFs where mode width is approximately less than $\approx 5\lambda$.

A. Impact of the index difference in the disordered waveguide

The results shown in Fig. 4 are for the waveguide index difference of $\Delta n_{\text{core}} = 0.01$ ($n_0 = 1.49$ and $n_1 = 1.50$). If the index difference is increased, the stronger transverse scattering should result in stronger transverse localization and smaller localized mode width values. This can be seen by plotting the PDF for the higher index difference of $\Delta n_{\text{core}} = 0.02$ ($n_0 = 1.48$ and $n_1 = 1.50$) in Fig. 5 and its magnified inset. The small mode width peak of the PDF relating to the Anderson localized modes in Fig. 5 has shifted to lower mode width values compared with Fig. 4 because of the larger Δn and stronger transverse scattering. Also, the convergence of the PDF hap-

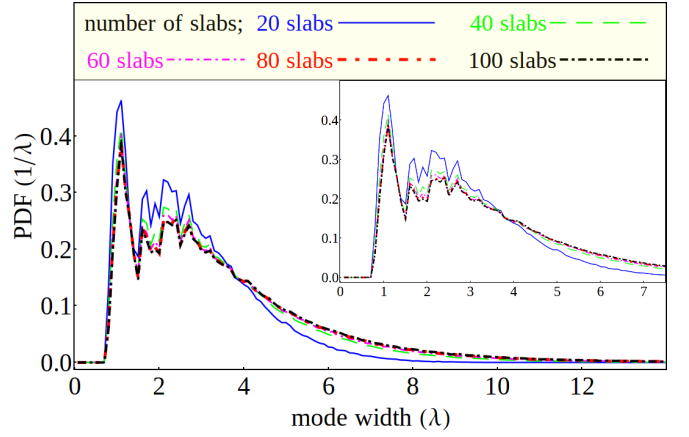


FIG. 5. $\Delta n_{\text{core}} = 0.02$ is increased in comparison to Fig. 4; The small-mode-width peak of the PDF shifts towards smaller mode width values indicating a stronger localization for a larger index contrast in the disordered waveguide. A magnified version is shown as an inset. $N_{\text{sat}} \approx 40$ is smaller for a stronger transverse scattering.

pens with a smaller number of slabs, i.e., N_{sat} is smaller when Δn is larger. Otherwise, the qualitative behavior of the PDFs are similar in the sense that the both waveguides support localized and extended modes simultaneously.

B. Impact of the boundary index difference

In the previous figures (Figs. 4, 5), the refractive index of the cladding n_c is assumed to be the same as the refractive index n_0 of the lower index layers. For the practical 2D disordered optical fiber of Ref.³⁷, the cladding of the structure is air with a refractive index of $n_c = 1$, which is considerably smaller than the lower index $n_0 = 1.49$ of the fiber. The cladding index of the fiber can be controlled by an additional cladding layer or an index matching gel. As such, understanding the impact of the refractive index of the boundary on the guided mode structure of the disordered waveguide is of practical importance. A lower cladding index increases the effective V-number of the whole disordered waveguide, resulting in an increase in the total number of modes. In this section, we will investigate the impact of the cladding refractive index on the distribution of the localized and extended modes, as well as on the scaling and eventual convergence of the mode-width PDF with the transverse size of the waveguide. Moreover, we will show that the impact of changing the cladding index is primarily on the extended modes, while the localized modes are hardly affected by changes in the cladding index step.

In Fig. 6, we consider a disordered waveguide with $\Delta n_{\text{core}} = 0.01$ ($n_0 = 1.49$ and $n_1 = 1.50$) and $\Delta n_{\text{clad}} = 0.01$ where $\Delta n_{\text{clad}} = n_0 - n_c$. This waveguide is identical in structure to that of Fig. 4 except for Δn_{clad} . The main difference between Fig. 6 and Fig. 4 is in the distribution

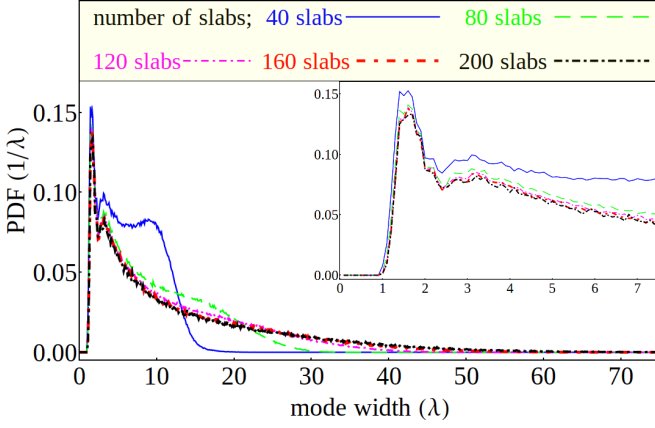


FIG. 6. Mode-width PDF of a disordered waveguide defined as $\Delta n_{\text{core}} = 0.01$, $\Delta n_{\text{clad}} = 0.01$, and $N = 40, 80, 120, 160, 200$ slabs. A lower cladding index significantly changes the distribution of the extended modes and PDF saturates at a much larger value of N ($N_{\text{sat}} \approx 160$). The inset represents a magnified version. A smaller cladding index only affects the extended mode width distribution, while the localized modes remain nearly unaffected.

of the extended modes. The presence of a larger cladding index difference in Fig. 6 results in a greater number of extended modes which appears as a large bump in the PDF for $N = 40$ slabs and smooths down when the PDF saturates to the terminal shape for large N . Another important difference between Fig. 6 and Fig. 4 is that the convergence of the PDF in Fig. 6 (larger Δn_{clad}) happens at a larger value of N . The inset in Fig. 6 ($\Delta n_{\text{clad}} = 0.01$) shows the same PDF magnified over the region of small mode width near the localized modes and should be compared with the inset in Fig. 4 ($\Delta n_{\text{clad}} = 0$). While the two figures are visually similar, the localized peak of Fig. 4 is observed to be clearly higher when comparing the vertical scales of the PDF plots. This is due to the fact that the total area under PDF is normalized to unity and the larger number of extended modes in Fig. 6 results in a reduction in the overall amplitude of the PDF over the entire domain. As such, the PDF in its present form cannot provide a fair comparison between the localized mode structure of Fig. 6 and Fig. 4. We will get back to this important point later in this section.

In Fig. 7 and Fig. 8 we investigate the effect of further lowering n_c to have $\Delta n_{\text{clad}} = 0.02$ and $\Delta n_{\text{clad}} = 0.04$, respectively. The insets are the magnified versions as before over the region of small mode width near the localized modes. We observe a trend similar to the comparison that we conducted above between Fig. 6 and Fig. 4. Therefore, we conclude that increasing the cladding index results in an increase in the number of extended modes, emphasizing that we have yet to show in this section that the localized modes are not affected by the change in the cladding index. Moreover, an increase in the cladding index difference results in a delayed convergence of the PDF to its terminal form resulting in a larger value of

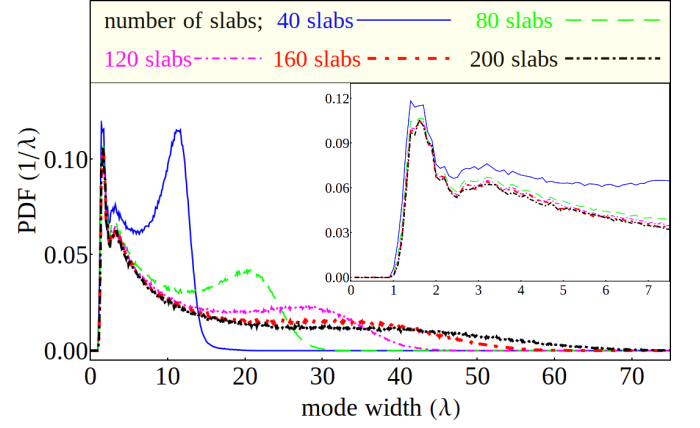


FIG. 7. The same as Fig. 6 except $\Delta n_{\text{clad}} = 0.02$. The PDF saturates to its terminal shape at a larger number of slabs ($N_{\text{sat}} \approx 200$). The inset is a magnified version.

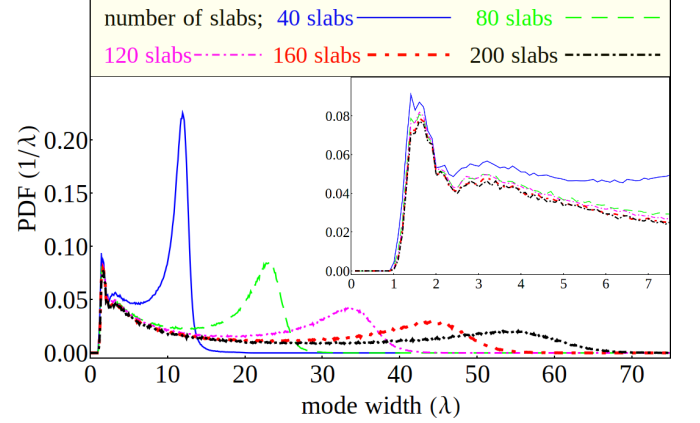


FIG. 8. The same as Fig. 6 except $\Delta n_{\text{clad}} = 0.04$. Further decreasing the cladding index delays the saturation of the PDF to larger values of N ($N_{\text{sat}} \gg 200$). The inset is a magnified version.

N_{sat} . In fact, it can be seen that $N_{\text{sat}} \approx 200$ for Fig. 7 and $N_{\text{sat}} \gg 200$ for Fig. 8.

Our discussion will not be complete without discussing the reverse effect of raising n_c above n_0 , hence a negative value of $\Delta n_{\text{clad}} = -0.005$. Of course, we assume that $n_c < n_1$; otherwise, no guiding mode would exist. Figure 9 ($\Delta n_{\text{clad}} = -0.005$) can best be compared with Fig. 4 with $\Delta n_{\text{clad}} = 0$. It is clear that raising n_c above n_0 (negative Δn_{clad}) removes a considerable number of extended modes from the system. Recall that the PDF in Fig. 4 showed two distinct peaks in the region near the localized modes and raising n_c above n_0 appears to remove the second localized peak (with a larger mode width). Therefore, we conclude that a negative Δn_{clad} not only removes many of the extended modes, it also removes those more weakly localized modes associated with the second peak in Fig. 4.

Previously in this Section, we mentioned that it is hard to judge the impact of the cladding refractive index on

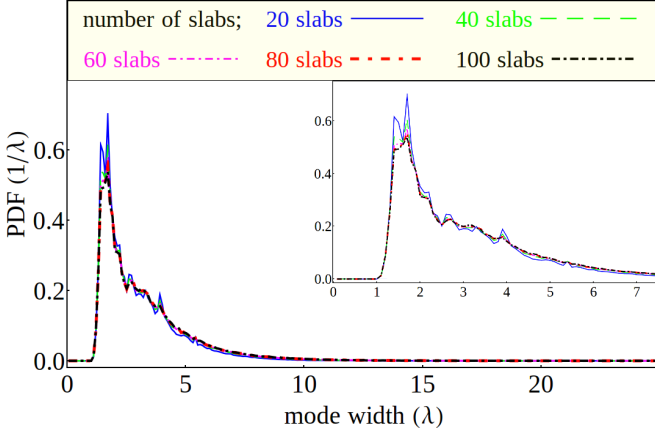


FIG. 9. The same as Fig. 4 except $\Delta n_{\text{clad}} = -0.005$. A cladding index larger than n_0 not only reduces the probability density of the extended modes, but also diminishes the second peak of the localized regime. The inset represents a magnified version.

the width distribution of the localized modes by comparing the PDFs from two different waveguides. The reason is that the total area under PDF is normalized to unity and different waveguide parameters result in different number of modes. As such, we need to come up with a method to clearly differentiate between the impact of the cladding index on the extended modes versus localized modes across different lattice parameters. In order to do this, it is best to use the *normalized PDF* which is the PDF multiplied by a constant factor such that total area under the normalized PDF curve equals the average number of modes in each class of random waveguide.

In Fig. 10, we plot the normalized PDF for disordered waveguides with $\Delta n_{\text{core}} = 0.01$ ($n_0 = 1.49$ and $n_1 = 1.50$), $d = \lambda$, and $N = 200$ slabs. Different curves in Fig. 10 correspond to different values of Δn_{clad} ranging from -0.005 to 0.04 . The curves belonging to the largest three values of Δn_{clad} are not fully saturated to the terminal PDF because $N = 200$ is smaller than N_{sat} in these cases, hence resulting in a bump in the extend mode region. The inset shows the magnified version of the same figure in the region of the localized modes. Figure 10 clearly shows that increasing the cladding index step merely introduces new extended modes and the localized modes are hardly affected. We re-emphasize the utility of the normalized PDF in revealing this important behavior. The case of $\Delta n_{\text{clad}} = -0.005$ is quite interesting, as it can be seen that raising n_c above n_0 strongly decouples extended modes and trims the large-mode-width edge of the localized mode region of the PDF. Therefore, if having more localized modes versus extended modes is a desired outcome of a design, a small or even negative Δn_{clad} is preferable.

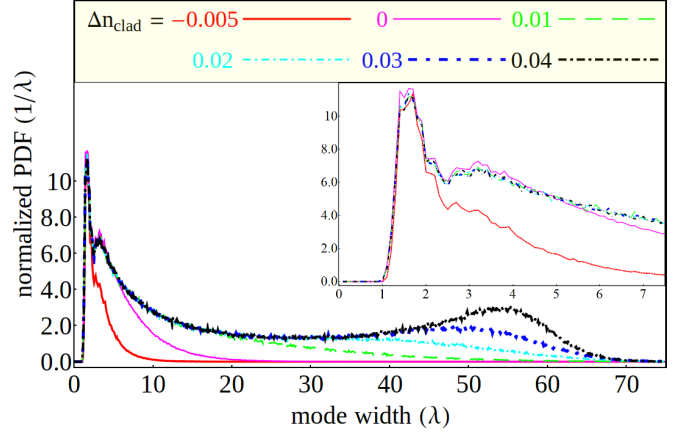


FIG. 10. Normalized PDF for disordered waveguides defined by $\Delta n_{\text{core}} = 0.01$, $N = 200$, and $\Delta n_{\text{clad}} = -0.005, 0.01, 0.02, 0.03$, and 0.04 . The magnified inset clearly shows that the statistics of the localized modes is independent of the cladding index unless for a negative Δn_{clad} .

C. Impact of the unit slab thickness

In the previous sections, we learned much about the behavior of the mode-width PDF for various refractive index configurations in the core and cladding. In all previous simulations, we assumed that the width of each slab is equal to the wavelength $d = \lambda$. However, the mode-width PDF depends on the value of d as well. Understanding the behavior of the mode-width PDF as a function of d is quite important because d is a parameter that can be used to optimize the disordered lattice given an objective function. For example, our objective can be to obtain the smallest possible mean value of the mode width calculated using the PDF, where d in addition to the refractive indexes can be used as an optimization parameter. In Figs. 11 and 12 we plot the normalized PDFs for disordered lattices defined by $n_c = n_0 = 1.49$, and $n_1 = 1.50$. The value of the unit slab thickness is different in each case, taking the values ranging over $d = 0.5\lambda - 2.5\lambda$, while keeping the total waveguide size equal to 200λ . Therefore, the case with $d = 0.5\lambda$ corresponds to $N = 400$, while the case with $d = 2\lambda$ corresponds to $N = 100$. As we discussed before, the normalized PDF integrates to the total number of modes, which varies from an average of 49 modes for the case of $d = 0.5\lambda$ to an average of 39 modes for the case of $d = 2.5\lambda$. In Fig. 11, it is clear that $d = 0.5\lambda$ corresponds to a normalized mode-width PDF with a long tail in the extended mode region. When d is increased to $d = \lambda$ and further to $d = 1.5\lambda$, the extended tail is gradually lowered contributing more to the localized region. It seems as if that the extended modes trade off their role with the localized modes of the second PDF hump. Another important observation is that the localized peak shifts slightly towards the smaller mode width values as the unit slab thickness increases.

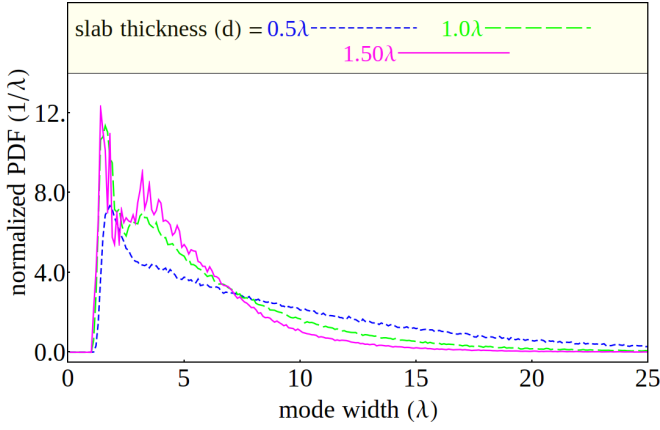


FIG. 11. Normalized mode-width PDF of disordered waveguides defined by $\Delta n_{\text{core}} = 0.01$, $\Delta n_{\text{clad}} = 0$, $N = 200$, and unit slab thickness of $d = 0.5, 1.0$, and 1.5λ . Overall, the waveguides show stronger localization for a thicker unit slab.

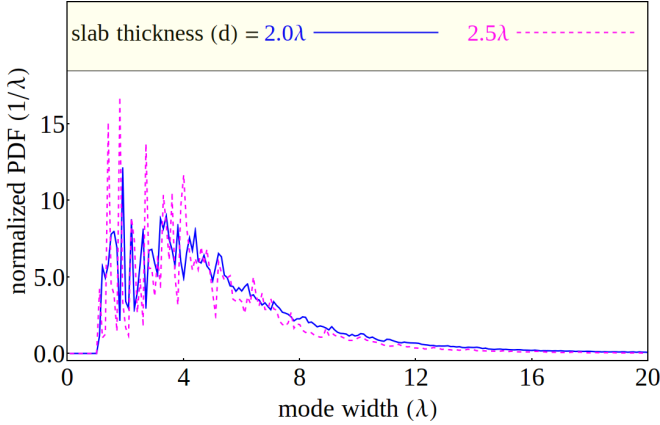


FIG. 12. The same as Fig. 11, except that the thickness of the unit slabs in the structure of the disordered waveguides is larger. The formation of local waveguides leads to sharp discrete peaks in the normalized PDF.

In Fig. 12, the normalized PDFs for disordered lattices with $d = 2\lambda$ and $d = 2.5\lambda$ are shown. The normalized PDF in these figures exhibit sharp peaks, which are markedly different from the PDFs we have observed in previous figures. Below, we will argue that these sharp peaks are mainly due to step-index waveguiding behavior of individual discrete waveguides formed in the random structure, rather than the Anderson localized modes. In order to understand this, consider the case of $d = 2\lambda$, where discrete local waveguides of widths $t = 2\lambda$, $t = 4\lambda$, $t = 6\lambda$, etc appear, respectively, with decreasing probability. The V-number of the slab waveguide is given by

$$V = \frac{\pi t}{\lambda} \sqrt{n_1^2 - n_0^2}, \quad (3)$$

which is equal to 1.09 for $t = 2\lambda$ and is proportionally larger for $t = 4\lambda$, $t = 6\lambda$, etc. We recall that the single-mode cut-off condition for the TE modes of a slab waveguide is $V = \pi/2$. Therefore, $t = 2\lambda$ is near cut-off and

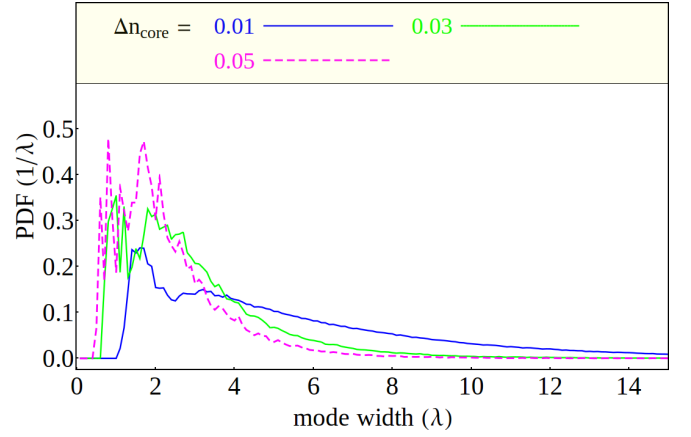


FIG. 13. The unit slab thickness is fixed at $d = \lambda$ but $\Delta n_{\text{core}} = 0.01, 0.03$, and 0.05 . As Δn_{core} increases, more local waveguides form in the structure and the PDF becomes more discrete.

$t = 4\lambda$ or larger are multimode. The large V-number in these waveguides results in highly confined modes that cannot interact with the modes of the neighboring waveguides to allow for randomized interaction to form Anderson localized modes. Therefore, in addition to the extended modes and the Anderson localized modes that stem from the more-loosely-bound modes, we encounter the regular step-index waveguiding modes in the form of sharp discrete peaks. The peaks are centered at mode-width values of the corresponding waveguides of discrete thickness values of $t = 2\lambda$, $t = 4\lambda$, $t = 6\lambda$, etc. The decreasing values of the discrete peaks in the PDF are indicative of the decreasing probability of having local waveguides with $t = 2\lambda$, $t = 4\lambda$, $t = 6\lambda$, etc, respectively. This situation is even more prominent in the case of $d = 2.5\lambda$, where discrete local waveguides have widths of $t = 2.5\lambda$, $t = 5\lambda$, $t = 7.5\lambda$, etc.

Our argument in the previous paragraph was based on the value of the V-number created in the locally formed waveguides. Therefore, if the refractive index contrast Δn_{core} is increased, we should observe a similar behavior, where narrow peaks related to regular step-index waveguiding modes should appear alongside with the extended modes and the Anderson localized modes. The discrete peaks in the PDF observed in Fig. 5 are in fact of this nature. In order to see this more clearly, in Fig. 13 we study the impact of increasing the value of the waveguide index difference Δn_{core} by comparing the mode-width PDFs for $\Delta n_{\text{core}} = 0.01$, $\Delta n_{\text{core}} = 0.03$, and $\Delta n_{\text{core}} = 0.05$, all for $d = \lambda$. Sharp peaks clearly appear when the refractive index contrast is increased.

The results presented in this section so far give a thorough overview on the statistical behavior of Anderson localized modes, extended modes, and regular step-index waveguiding modes, all of which can be present in a disordered waveguide at the same time.

We conclude this manuscript by visualizing the interplay between the impact of the localized and extended

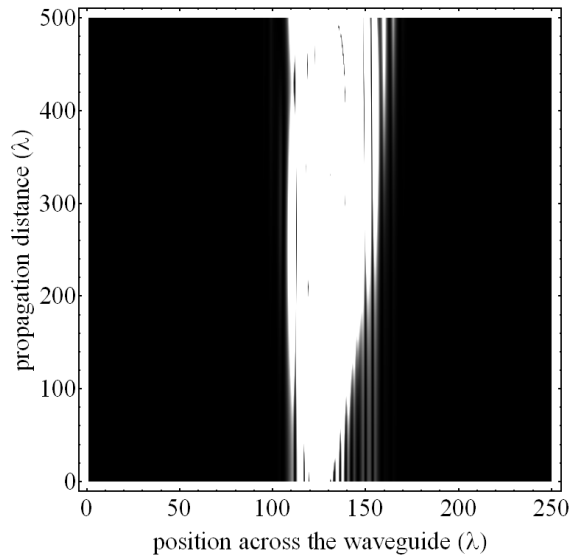


FIG. 14. Propagation of a Gaussian beam ($\omega = 3\lambda$) along a disordered waveguide defined by $\Delta n_{\text{core}} = 0.01$, $\Delta n_{\text{clad}} = 0$, and $N = 200$. The beam eventually localizes to a relatively stable width after an initial expansion.

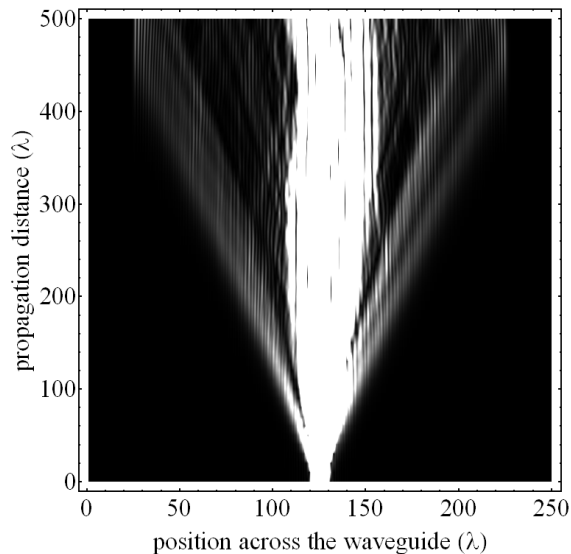


FIG. 15. The refractive index profile of the disordered waveguide is exactly the same as Fig. 14, except $\Delta n_{\text{clad}} = 0.04$. Formation of the extended modes generates a background noise.

modes in a disordered waveguide. In Fig. 14, we numerically simulate the propagation of light in a disordered waveguide and plot the intensity distribution of the guided beam as it propagates along the waveguide.

The disordered waveguide is defined with $N = 200$ slabs, where each slab's thickness is $d = \lambda$, and the refractive indexes are given by $n_1 = 1.5$ and $n_0 = 1.49$. The cladding index in Fig. 14 is $n_c = 1.49$, so $\Delta n_{\text{clad}} = 0$, while the cladding index in Fig. 15 is $n_c = 1.45$ resulting in $\Delta n_{\text{clad}} = 0.04$. Based on the results of the previous section and the discussion on the normalized mode-width PDF, we expect to have nearly identical distribution of localized modes. However, the larger value of Δn_{clad} in Fig. 15 results in a larger number of extended modes.

In Figs. 14 and 15, the injected beam is a Gaussian characterized by the electric field distribution of the form $E(x) \propto \exp(-x^2/\omega^2)$ with $\omega = 3\lambda$ at the entrance, where x is the coordinate across of the waveguide. The center of the Gaussian beam is assumed to be in the middle of the disordered lattice. In the single realization of the disordered waveguide shown in Fig. 14 with very few extended modes, there is virtually no background noise and the initial excitation is clearly Anderson localized after a short propagation distance. However, in the presence of a large number of extended modes in Fig. 15, a background noise due to extended modes is evident throughout the propagation, while the Anderson localized modes still play a prominent role in the center that is similar to the one observed in Fig. 14.

IV. CONCLUSION

In this manuscript, we have introduced the mode-width PDF as a powerful tool to study the transverse Anderson localization properties of guided modes of a disordered one dimensional optical waveguide. The mode-width PDF has been used for detailed statistical analysis of the impact of various structural and optical parameters of the disordered waveguide. A disordered waveguide supports both Anderson localized modes as well as extended modes. The mode-width PDF sheds light into the distribution of these modes and provides a powerful framework to manipulate such distributions, for example to quench the number of extended modes while minimally affecting the localized ones. An important observation in this manuscript is the convergence of the mode-width PDF to a terminal configuration as a function of the transverse dimension of the disordered waveguide. This has been shown by performing a scaling analysis of the mode-width PDF and can be quite helpful in turning a formidable computational problem from nearly impossible to a tractable one. The results presented in the manuscript are intended to establish the framework for a comprehensive analysis of the mode-width statistics for 2D transverse Anderson localization in optical fibers in the future.

* mafi@unm.edu

¹ P. W. Anderson, "Absence of diffusion in certain random lattices," Phys. Rev., **109**, 1492–1505 (1958).

- ² E. Abrahams, “50 years of Anderson localization,” (World Scientific, 2010).
- ³ M. Segev, Y. Silberberg, and D. N. Christodoulides, “Anderson localization of light,” *Nature Photonics* **7**, 197–204 (2013).
- ⁴ R. L. Weaver, “Anderson localization of ultrasound,” *Wave Motion*, **12**, 129–142 (1990).
- ⁵ I. S. Graham, L. Piche, M. Grant, “Experimental evidence for localization of acoustic waves in three dimensions,” *Phys. Rev. Lett.* **64**, 3135–3138 (1990).
- ⁶ R. Dalichaouch, J. P. Armstrong, S. Schultz, P. M. Platzman, and S. L. McCall, “Microwave localization by two-dimensional random scattering,” *Nature*, **354**, 53–55 (1991).
- ⁷ S. John, “Electromagnetic absorption in a disordered medium near a photon mobility edge,” *Phys. Rev. Lett.* **53**, 2169–2172 (1984).
- ⁸ S. John, “Strong localization of photons in certain disordered dielectric superlattices,” *Phys. Rev. Lett.* **58**, 2486–2489 (1987).
- ⁹ S. John, “Localization of light,” *Phys. Today*, **44**, 32–40 (1991).
- ¹⁰ P. W. Anderson, “The question of classical localization: A theory of white paint?,” *Philos. Mag. B*, **52**, 505–509 (1985).
- ¹¹ A. D. Lagendijk, B. V. Tiggelen, B., D. S. Wiersma, “Fifty years of Anderson localization,” *Phys. Today*, **62**, 24–29 (2009).
- ¹² H. Hu, A. Strybulevych, J. H. Page, S. E. Skipetrov, and B. A. van Tiggelen, “Localization of ultrasound in a three-dimensional elastic network,” *Nature Physics* **4**, 945–948 (2008).
- ¹³ A. A. Chabanov, M. Stoytchev, and A. Z. Genack, “Statistical signatures of photon localization,” *Nature*, **404**, 850–853 (2000).
- ¹⁴ J. Billy, V. Josse, Z. Zuo, A. Bernard, B. Hambrecht, P. Lugan, D. Clément, L. Sanchez-Palencia, P. Bouyer, and A. Aspect, “Direct observation of Anderson localization of matter waves in a controlled disorder,” *Nature* **453**, 891–894 (2008).
- ¹⁵ Y. Lahini, Y. Bromberg, D. N. Christodoulides, and Y. Silberberg, “Quantum correlations in two-particle Anderson localization,” *Phys. Rev. Lett.* **105**, 163905 (2010).
- ¹⁶ C. Thompson, G. Vemuri, and G. S. Agarwal, “Anderson localization with second quantized fields in a coupled array of waveguides,” *Phys. Rev. A* **82** 053805 (2010).
- ¹⁷ Y. Lahini, Y. Bromberg, Y. Shechtman, A. Szameit, D. N. Christodoulides, R. Morandotti, and Y. Silberberg, “Hanbury Brown and Twiss correlations of Anderson localized waves,” *Phys. Rev. A* **84**, 041806(R) (2011).
- ¹⁸ A. F. Abouraddy, G. Di Giuseppe, D. N. Christodoulides, and B. E. A. Saleh, “Anderson localization and colocalization of spatially entangled photons,” *Phys. Rev. A* **86** 040302(R) (2012).
- ¹⁹ S. S. Abdullaev, and F. K. Abdullaev, “On propagation of light in fiber bundles with random parameters,” *Radiofizika* **23**, 766–767 (1980).
- ²⁰ H. de Raedt, A. D. Lagendijk, and P. de Vries, “Transverse localization of light,” *Phys. Rev. Lett.* **62**, 47–50 (1989).
- ²¹ T. Schwartz, G. Bartal, S. Fishman, and M. Segev, “Transport and Anderson localization in disordered two-dimensional photonic lattices,” *Nature* **446**, 52–55 (2007).
- ²² A. Mafi, “Transverse Anderson localization of light: a tutorial,” *Adv. Opt. Photon.* **7**, 459–515 (2015).
- ²³ Y. Lahini, A. Avidan, F. Pozzi, M. Sorel, R. Morandotti, D. N. Christodoulides, and Y. Silberberg, “Anderson Localization and Nonlinearity in One-Dimensional Disordered Photonic Lattices,” *Phys. Rev. Lett.* **100**, 013906 (2008).
- ²⁴ L. Martin, G. D. Giuseppe, A. Perez-Leija, R. Keil, F. Dreisow, M. Heinrich, S. Nolte, A. Szameit, A. F. Abouraddy, D. N. Christodoulides, and B. E. A. Saleh, “Anderson localization in optical waveguide arrays with off-diagonal coupling disorder,” *Opt. Express*, **19**, 13636–13646 (2011).
- ²⁵ S. Karbasi, C. R. Mirr, P. G. Yarandi, R. J. Frazier, K. W. Koch, and A. Mafi, “Observation of transverse Anderson localization in an optical fiber,” *Opt. Lett.* **37**, 2304–2306 (2012).
- ²⁶ S. Karbasi, C. R. Mirr, Ry. J. Frazier, P. G. Yarandi, K. W. Koch, and A. Mafi, “Detailed investigation of the impact of the fiber design parameters on the transverse Anderson localization of light in disordered optical fibers,” *Opt. Express* **20**, 18692–18706 (2012).
- ²⁷ S. Karbasi, T. Hawkins, J. Ballato, K. W. Koch, and A. Mafi, “Transverse Anderson localization in a disordered glass optical fiber,” *Opt. Mat. Express* **2**, 1496–1503 (2012).
- ²⁸ S. Karbasi, R. J. Frazier, K. W. Koch, T. Hawkins, J. Ballato, and A. Mafi, “Image transport through a disordered optical fibre mediated by transverse Anderson localization,” *Nature Communications* **5**, 3362 (2014).
- ²⁹ S. Karbasi, K. W. Koch, and A. Mafi, “Image transport quality can be improved in disordered waveguides,” *Opt. Commun.* **311**, 72–76 (2013).
- ³⁰ T. A. Lenahan, “Calculation of Modes in an Optical Fiber Using the Finite Element Method and EISPACK,” *Bell System Technical Journal*, **62**, 2663–2694 (1983).
- ³¹ R. G. S. El-Dardiry, S. Faez, and Ad. Lagendijk, “Snapshots of Anderson localization beyond the ensemble average,” *Phys. Rev. B* **86**, 125132 (2012).
- ³² Y. V. Kartashov, V. V. Konotop, V. A. Vysloukh, and L. Torner, “Light localization in nonuniformly randomized lattices,” *Opt. Lett.* **37**, 286288 (2012).
- ³³ B. Abaie, and A. Mafi, “Modal analysis of transverse Anderson localization near the boundary of a one-dimensional disordered optical lattice,” in *Frontiers in Optics 2015 OSA Technical Digest* (online) (Optical Society of America, 2015), paper JT4A.76.
- ³⁴ B. Abaie, S. R. Hosseini, S. Karbasi, and A. Mafi, “Modal analysis of the impact of the boundaries on transverse Anderson localization in a one-dimensional disordered optical lattice,” *Opt. Comm.*, **365**, 208–214 (2016).
- ³⁵ W. P. Huang and C. L. Xu, “Simulation of three-dimensional optical waveguides by full-vector beam propagation method,” *J. Lightwave Technol.* **29** 2639–2649 (1993).
- ³⁶ S. Karbasi, K. W. Koch, and A. Mafi, “Modal perspective on the transverse Anderson localization of light in disordered optical lattices,” *J. Opt. Soc. Am. B* **30**, 1452–1461 (2013).
- ³⁷ S. Karbasi, R. J. Frazier, C. R. Mirr, K. W. Koch, and A. Mafi, “Fabrication and characterization of disordered polymer optical fibers for transverse Anderson localization of light,” *J. Vis. Exp.* **77** (2013).